

# Structure of the Crystalline C<sub>60</sub> Photopolymer and the Isolation of Its Cycloadduct Components

Éva Kováts, Gábor Oszlányi, and Sándor Pekker\*

Research Institute for Solid State Physics and Optics, Hungarian Academy of Sciences, P.O. Box 49, H-1525 Budapest, Hungary

Received: April 5, 2005; In Final Form: May 3, 2005

We produced C<sub>60</sub> photopolymer in gram quantity by a new monomer recycling method and extracted its soluble components. The most abundant components, the (2 + 2) cycloadduct dimer, C<sub>120</sub>, and several oligomers were isolated by high-performance liquid chromatography (HPLC). Three different C<sub>180</sub> isomers were identified on the basis of their formation and decomposition reactions. The crystal structure of the insoluble photopolymer is face-centered cubic (fcc) with a contracted lattice parameter relative to the pristine C<sub>60</sub>. The lattice parameter and the amounts of soluble oligomers depend on the preparation temperature. We explain this variation with a topochemical model of photopolymerization: The geometrical conditions allow the formation of only linear or planar oligomers in the triangular or square sublattices. Competing reactions in the intersecting planes prevent the formation of large oligomers. The lattice contraction is proportional to the number of cycloadduct bonds.

## 1. Introduction

Photopolymerization of fullerenes was first demonstrated by Rao et al.,<sup>1</sup> who transformed a thin film of C<sub>60</sub> into a polymerized derivative by illuminating it with UV and visible light in inert atmosphere. The mechanism of the reaction proved to be a photochemical (2 + 2) cycloaddition<sup>2</sup> with the formation of four-membered rings between adjacent C<sub>60</sub> balls. The possible existence of covalent interfullerene bonds initiated a series of extended studies leading to the discovery of various neutral and ionic fullerene polymers.<sup>3</sup> While high-pressure and ionic polymerizations were performed on bulk samples, early photopolymerization studies were restricted to thin films and single-crystal surfaces, since the strong absorption of both C<sub>60</sub> and its photopolymer prevented further reaction in the depths more than a micrometer. Despite the microgram quantities of available samples, some of the most important molecular properties of the photopolymer were revealed within a short time. A series of (C<sub>60</sub>)<sub>n</sub> clusters (*n* < 20) were detected by laser desorption mass spectrometry.<sup>1</sup> These clusters support the polymerization, although they may not reflect the original structure of the photopolymer because both fragmentation and polymerization can take place during the desorption.<sup>1</sup> The formation of covalent bonds was evidenced by infrared and Raman spectroscopic methods<sup>1,4</sup> detecting the symmetry lowering of C<sub>60</sub> balls due to the cycloaddition. The kinetics of the photopolymerization<sup>2,3,5–7</sup> and the thermal degradation<sup>8</sup> were developed by spectroscopic methods. Theoretical calculations determined the stability and molecular geometry of various (2 + 2) cycloadduct oligomers and polymers<sup>9–15</sup> and supported Raman evidence<sup>16,17</sup> that photopolymers are mixtures of short oligomers. However, the bulk structure of photopolymerized C<sub>60</sub> remained controversial: atomic force microscopy on crystalline photopolymer films showed a characteristic herringbone pattern<sup>18</sup> as a sign of ordered arrays of linear oligomers; powder X-ray diffraction showed a contracted face-centered cubic (fcc) cell<sup>1</sup> excluding linear

oligomers; and X-ray photoelectron spectroscopy suggested a rhombohedral structure for highly polymerized crystalline films.<sup>19</sup> Detailed studies of bulk samples would be important to understand the intrinsic structure and properties of the photopolymer. Sun et al.<sup>20</sup> performed the first large-scale photopolymerization of C<sub>60</sub> and C<sub>70</sub> in stable toluene/acetonitrile colloidal dispersions of the fullerenes. The typically 100 nm particle size made possible a complete polymerization of C<sub>60</sub>, resulting in a yield of 10 mg. The materials were characterized by various spectroscopic methods.<sup>20,21</sup> Recently, Cataldo succeeded in the photopolymerization of a similar quantity of C<sub>60</sub> in various halogenated solvents.<sup>22,23</sup> Pusztai et al.<sup>24</sup> illuminated high-surface-area powders of C<sub>60</sub> with UV and visible light and obtained 10 mg of microcrystalline photopolymer. Pusztai et al.<sup>24</sup> observed the contraction of the fcc lattice by X-ray diffraction and determined the heat of depolymerization by differential scanning calorimetry. To explain the variation of the lattice parameter, they suggested the formation of small ring-shaped oligomers such as triangle and square. In the meantime, the smaller cycloadduct oligomers of C<sub>60</sub> were prepared by other methods<sup>25–29</sup> and the structures of the dimer and a few trimers were characterized.<sup>30–33</sup>

Recently, we worked out a new monomer recycling method for the photopolymerization of C<sub>60</sub> and increased the yield up to one gram.<sup>34</sup> The large amount of the photopolymer made possible the extraction of its soluble components. Preliminary structural studies indicated that the extracts were mixtures of oligomers.<sup>34,35</sup> We isolated the cycloadduct dimer by selective crystallization.<sup>35</sup> In this paper we summarize the recent developments of our preparation method, describe the isolation of cycloadduct oligomers by high-performance liquid chromatography (HPLC) and suggest a topochemical model for the photopolymerization.

## 2. Experimental Section

We performed the bulk photopolymerization of C<sub>60</sub> via a monomer recycling method, developed recently.<sup>34</sup> Typically, a

\* Corresponding author. E-mail: pekker@szfki.hu.

rough suspension of solid  $C_{60}$  powder (1 g) in its saturated toluene solution (20 mL) was sealed in a Pyrex tube and illuminated with two 23 W luminescent light sources. The temperature of polymerization was controlled by air cooling in the range 40–110 °C. Due to the nonuniform illumination, a temperature gradient formed along the tube, resulting in a thermal convection of the suspension and inducing a continuous dissolution–recrystallization of  $C_{60}$ . Thus, the surface of the monomer was refreshed, retaining steady state conditions of the polymerization for a long time. While the liquid state transport recycled the monomer, the practically insoluble polymer accumulated gradually in the solid phase. The reaction mixture was homogenized by sonication occasionally. After a few weeks, the reaction was stopped and the products were purified and processed.

The as-prepared photopolymer samples were extracted in various organic solvents. To separate the unreacted  $C_{60}$  from the polymer, the first extractions were carried out in hexane. We considered the residue insoluble in hexane as the raw photopolymer and extracted its soluble components in toluene and 1-methylnaphthalene subsequently. The final extraction steps were assisted by intensive sonication.

The extracted mixtures were separated by a Jasco LC-1500 HPLC system equipped with a UV–visible detector, an analytical (4.6 mm  $\times$  250 mm) and a semipreparative (10 mm  $\times$  250 mm) Cosmosil “Buckyprep” column, and an Advantec SF-2100W fraction collector. Chromatograms were detected at 330 nm. We applied various compositions of toluene/methylnaphthalene eluents. After purification, the higher-amount fractions were crystallized from toluene in a rotary evaporator.

X-ray powder diffraction of the insoluble polymer and the precipitated oligomer samples (5 mg, in glass capillaries) was conducted in transmission geometry with a Huber G670 Image Foil Guinier camera at a Cu  $K\alpha_1$  wavelength of 1.540 56 Å.

### 3. Results

Photopolymerization of  $C_{60}$  was performed at different temperatures and irradiation times. The overall yield of the raw photopolymer decreased from 67 to 9% when the polymerization temperature was increased from 40 to 110 °C. At the same time, the relative amounts of the soluble components increased significantly. The yield of the polymer did not correlate with the preparation time of 30–90 days, indicating that in this range the polymerization reaction reached its thermal equilibrium.

The compositions of the toluene and methylnaphthalene extracts of the photopolymers were analyzed by HPLC. Figure 1 shows a typical chromatogram taken in the toluene mobile phase. The chromatographic peaks observed at retention times (RTs) of 8, 20, 40–50, and 70–90 min correspond to the monomer ( $C_{60}$ ), the dimer ( $C_{120}$ ), various trimers ( $C_{180}$ ), and various tetramers ( $C_{240}$ ), as will be discussed below. In agreement with our preliminary results,<sup>34</sup> the composition of the extracts depended on the solvent, the extraction time and method, and the polymerization temperature. Hexane extracts contained only  $C_{60}$ , while the first toluene extracts were predominantly mixtures of  $C_{60}$  and its dimer with some traces of trimers. The amounts of trimers and tetramers increased significantly in the methylnaphthalene extracts; however, the monomer and the dimer were also observed at all steps of extraction (Figure 1). During the extraction, the relative amounts of the soluble components varied, resulting in a slight accumulation of trimers and tetramers in the final extracts. Sonication enhanced the rate of solubility without a significant influence on the composition. The extraction was stopped when

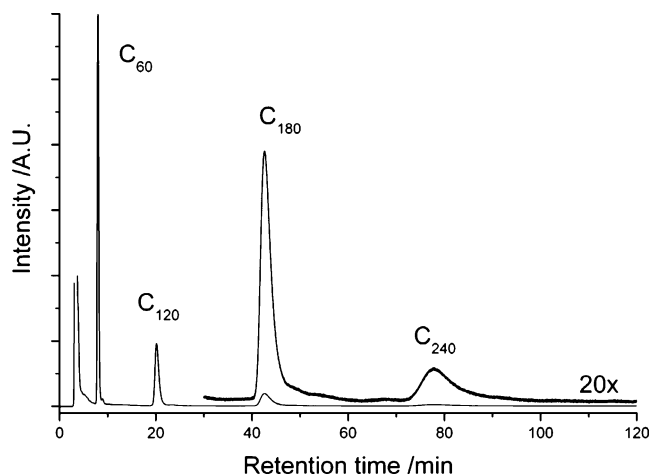


**Figure 1.** HPLC chromatogram of the soluble components of fullerene photopolymer extracted in 1-methylnaphthalene. Polymerization temperature, 100–110 °C; column, Cosmosil Buckyprep; elution, toluene 1 mL/min. Relative peak areas:  $C_{60}$ , 59%;  $C_{120}$ , 24%;  $C_{180}$ , 12%;  $C_{240}$ , 5%.

the concentration decreased about 1 order of magnitude despite intensive sonication.

To determine the degree of polymerization, the major soluble components of the photopolymers were separated and purified by semipreparative HPLC. Since the cycloadduct dimer ( $C_{120}$ ) was prepared previously by other methods<sup>25,26</sup> and its structure was determined,<sup>31</sup> we assigned the RT = 20 min peak as this dimer on the basis of its IR spectrum<sup>34</sup> by comparing it with those available in the literature.<sup>26,27</sup> Due to the significant difference of the retention times, the dimer was easily separated from  $C_{60}$  in toluene. After precipitation from toluene, crystalline  $C_{120}$  was obtained in 99.3% purity.

Prior to HPLC separation, the methylnaphthalene extracts were collected for a week to enrich the amounts of the less abundant trimers and tetramers. Instead of pure toluene, a 20% methylnaphthalene/toluene mobile phase was used to decrease the separation time and prevent the oligomers from decomposition. Previously, Komatsu et al.<sup>31</sup> found that the trimers of  $C_{60}$ , prepared by the mechanochemical method, decomposed in solution under ambient conditions in a few days. Despite the precautions, the separated oligomers at least partially decomposed in the dilute solutions and we could not obtain these materials in pure crystalline forms. However, the decomposition products gave evidence of the degree of polymerization of the parent oligomers. The materials corresponding to the RT = 40–50 min peaks partially decomposed to dimer and monomer during the HPLC separation. Upon heating the solution to 100 °C, the decomposition completed within a few hours. Since no decomposition products were observed other than the dimer and the monomer, we assigned these peaks as trimers.

The RT = 70–90 min peaks were assigned as tetramers by similar arguments: During HPLC collection, these materials decomposed to trimers, the dimer, and the monomer. Only traces of the parent peaks were observed after separation. Figure 2c shows a chromatogram of the trimers formed by the decomposition of the RT = 70–90 min peaks. In contrast to the three trimers of the starting extract (Figure 2a), only two peaks are observed here with significantly different intensities, showing their different origin. The high intensity of the RT = 47 min peak indicates that it formed from the most abundant (RT = 78 min) tetramer. A partial decomposition of this tetramer in the starting extract resulted in an accumulation of the RT = 47

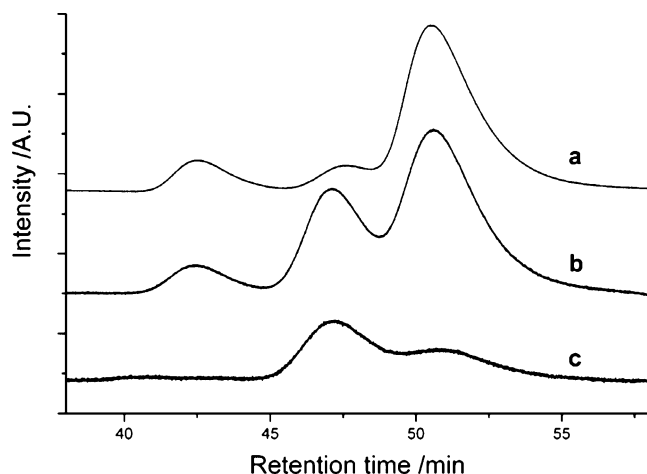


**Figure 2.** Trimer fractions of the HPLC chromatograms of fullerene photopolymer extracts: (a) freshly extracted in methylnaphthalene; (b) partially decomposed extract after 2 weeks of collection; (c) decomposition fragments of the tetramers separated previously by HPLC. Polymerization temperature, 55–65 °C; column, Cosmosil Buckyprep; elution, toluene 1 mL/min.

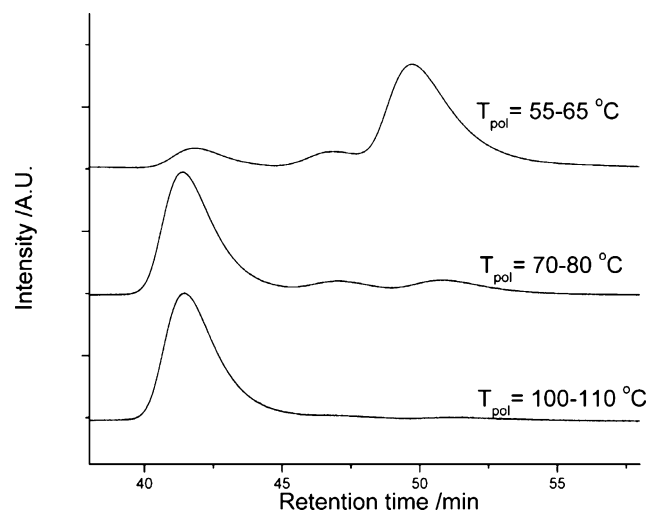


**Figure 3.** Trimer fractions of the HPLC chromatograms of fullerene photopolymers prepared at different temperatures. Column, Cosmosil Buckyprep; elution, toluene 1 mL/min.

min trimer during a week of sample collection, while the intensities of the RT = 41 and 50 min peaks did not change (Figure 2b).

Similar to the total amounts of soluble oligomers, the relative concentrations of their isomers depend strongly on the polymerization temperature. Figure 3 shows the detailed chromatograms of the trimers prepared at three different temperatures. Three peaks can be observed at RT = 41, 47, and 50 min, corresponding to different isomers. At polymerization temperatures below 70 °C, the RT = 50 min trimer formed abundantly, while, at higher temperatures, the RT = 41 min trimer became predominant. At 110 °C, only this trimer component formed in significant amount.

The photopolymers were crystalline with the cubic lattice parameter depending on the preparation conditions. The powder X-ray diffractograms of a typical insoluble photopolymer sample and the dimer precipitated from toluene are compared with that of C<sub>60</sub> in Figure 4. All diffractograms correspond to face-centered cubic (fcc) crystal structures with slightly different lattice parameters. The structural parameters of various samples are summarized in Table 1. The dimer exhibits broader lines and a contracted unit cell with a lattice parameter of  $a = 14.05$

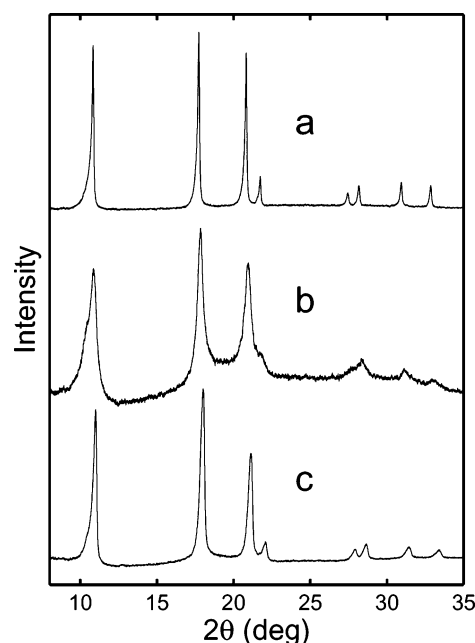


**Figure 4.** Powder X-ray diffractograms of (a) C<sub>60</sub> ( $a = 14.15$  Å), (b) C<sub>120</sub> crystallized from toluene ( $a = 14.05$  Å), and (c) an insoluble fraction of fullerene photopolymer prepared at 55–65 °C ( $a = 13.95$  Å).

Å relative to C<sub>60</sub>. The X-ray diffraction peaks of the polymers are only slightly broadened relative to C<sub>60</sub>, while the lattice parameters are further contracted depending on the polymerization temperature. The lower the polymerization temperature, the higher the contraction of the fcc lattice parameter (Table 1). In contrast to the dimer and the insoluble polymers, the precipitated mixtures of various oligomers were amorphous.

#### 4. Discussion

The X-ray diffraction data show that during photopolymerization the fcc structure of C<sub>60</sub> is preserved, while the lattice parameter decreases continuously in the 14.15–13.90 Å range. This structural change is consistent with the formation of a solid solution of randomly oriented molecules of various shapes and sizes. We explain the bulk photopolymerization of C<sub>60</sub> as a series of independent (2 + 2) cycloadditions controlled by the topochemical conditions of the fcc lattice. The first step is the formation of cycloadduct dimers. Considering the absorptivity of C<sub>60</sub> and the intensity of illumination, photoexcitation produces independent triplet state molecules<sup>5,6</sup> within a micron thick surface region. Each excited C<sub>60</sub> molecule can react with one of its 12 nearest neighbors in the fcc lattice, forming a dilute crystalline solution of C<sub>120</sub> molecules with the main axis oriented randomly. A similar disordered structure was also obtained with the high-pressure polymerization of C<sub>60</sub>.<sup>36</sup> As the concentration of the dimers increases, more and more C<sub>60</sub> can attach to dimers, forming trimers and finally higher oligomers. The molecular geometries of the possible oligomers are determined by the spatial orientation of the 30 double bonds of C<sub>60</sub> relative to the nearest neighbor directions. Since a basic requirement of the cycloaddition is the rectangular orientation of the four reacting atoms, only those double bonds can take part in a further reaction which faces the center of a nearest neighbor molecule.<sup>12</sup> We summarize in Figure 5 the possible trimers and tetramers that are compatible with the fcc structure. The 18 nearest neighbors of an isolated dimer make possible the formations of four isomers of trimer with center-to-center interfullerene angles of 60, 90, 120, and 180°. We did not consider the previously



**TABLE 1: Structural Characteristics of Crystalline C<sub>60</sub> and Its Photopolymers**

sample	preparation method	lattice parameter (Å)	average number of bonded neighbors ( $n_B$ )
monomer		14.15	0
dimer	monomer transport, recrystallized	14.05	1
polymer	monomer transport (80–110 °C)	13.95–14.00	2.0–1.5
polymer	monomer transport (40–65 °C)	13.93–13.95	2.3–2.0
polymer	powder method (<50 °C) <sup>24</sup>	13.90	2.6

suggested<sup>12,13</sup> 60° V-shaped trimer (and similarly the rectangular U-shaped tetramer) because the terminal C<sub>60</sub> units of these molecules satisfy the conditions of (2 + 2) cycloaddition and form the closed triangle (or square). Once a nonlinear trimer is formed, the centers of its three C<sub>60</sub> units determine either a square (100) or a triangular (111) plane of the lattice. Due to the orientation of double bonds, these trimers can only react with the C<sub>60</sub> molecules of the same planes. Thus, the formation of three-dimensional oligomers, suggested previously,<sup>16</sup> or an extended network is prevented. Such clusters would destroy the observed fcc lattice (Figure 4).

Planarity limits the maximum number of bonded neighbors ( $n_B$ ) to six in triangular planes and four in square planes. The growth of the oligomers is a competing process which keeps the oligomer content of the planes below the percolation limit: each C<sub>60</sub> unit can form oligomers in one of the three square planes and four triangular planes intersecting the same lattice site. At the final stage of polymerization, the cycloaddition may take place between the adjacent oligomers of the same planes. However, the oligomers belonging to the same planes have two different bond orientations, which cannot be attached to each other because the corresponding bonds do not form a rectangle. The origin of the two sets of bond orientations is the lack of 4-fold and 6-fold rotation axes in C<sub>60</sub>: The monomer units of the planar oligomers are oriented with either their C<sub>2</sub> or C<sub>3</sub> axis perpendicular to the square or the triangular planes, respectively (Figure 5). Each monomer unit of an oligomer has the same orientation. Individual rotation of the monomer units by 90° about C<sub>2</sub> or by 60° about C<sub>3</sub> creates the other set of orientation. Thus, cycloadduct bonds can form only between half of the adjacent oligomers that formed independently in the same plane, preventing the growth of extended two-dimensional polymeric regions. The small size of oligomers corresponds to a significantly lesser number of bonded neighbors than the possible maximum.

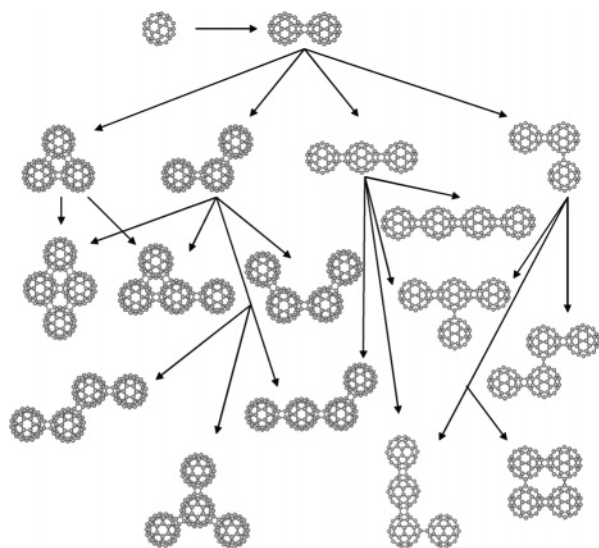


**Figure 5.** Derivation of the topochemically allowed cycloadduct trimers and tetramers of C<sub>60</sub> in the fcc lattice. Only one of the two different bond orientations or stereoisomers is shown.

Apart from the symmetry, the dimensional changes can control the growth of the oligomers. The formation of cycloadduct bonds is accompanied by a contraction of the distance between the reacting molecules along the new bonds. Considering the structural data of the cycloadduct dimer<sup>25</sup> and polymers<sup>3</sup>, the center-to-center distance of C<sub>60</sub> units decreases from  $r_0 = 10.0$  Å to  $r_B = 9.2$  Å when a bond is formed. The anisotropic contraction builds up an increasing stress between the growing molecule and its neighbors, hindering the growth of long linear extension oligomers. However, the more isometric oligomers, for example, curved, branched, or ring-shaped structures, can minimize the stress, preserving a disordered fcc structure.<sup>24</sup> Assuming that the cycloadduct bonds are randomly distributed along the 12 first neighbor directions,<sup>34,35</sup> the lattice parameter  $a$  can be expressed in terms of the average of the bonded ( $r_B$ ) and nonbonded distances ( $r_0$ ):

$$a = \frac{\sqrt{2}}{12}(n_B r_B + (12 - n_B)r_0) \quad (1)$$

Only the nonbonded distance of rotating C<sub>60</sub> molecules was considered here, because polymerization cannot take place in the orientationally ordered phase.<sup>2,7</sup> Apart from C<sub>60</sub>, it is the C<sub>120</sub> dimer phase for which independent experimental and calculated lattice parameters exist. The two values agree perfectly, which supports the disordered fcc structure and the use of eq 1. This disordered structure is unique in the sense that the lower symmetry dumbbell-shaped molecules form a high-symmetry fcc lattice. Previous crystallization of C<sub>120</sub> from 1,2-dichlorobenzene resulted in the formation of ordered single crystals of low symmetry and with some solvent included.<sup>25</sup> The driving force of the formation of the unusual disordered crystals may be the high orientational entropy ( $S = 1.26 \times 10^{-2}$  J/gK, when applying the lattice model of polymer systems<sup>37</sup>). Using the experimental lattice parameters, the average number of bonded neighbors ( $n_B$ ) can be calculated from eq 1. For insoluble photopolymers, prepared by the monomer transport method,  $n_B$  is 1.5–2.3, depending on the polymerization temperature (Table 1). Even the highest values are much less than those of surface layers,<sup>19</sup> showing the different structures of the bulk and surface polymers.

The strong influence of the polymerization temperature on the relative amounts of various trimers (Figure 3) can be explained by the different temperature dependence of the rates of their formation and decomposition. Since at lower polymerization temperatures the decomposition of the oligomers is negligible,<sup>8</sup> their relative amounts are controlled by the rates of formation. Under these conditions, the reaction of a dimer with one of its 18 nearest neighbor monomers results in ratios of 4:4:8:2 for the amounts of 60°, 90°, 120°, and 180° interfullerene angle trimers, respectively.<sup>12</sup> Considering the stress, which accompanies the formation of linear structures, the expected abundance of the 180° trimer is even less. Thus, we assume that the three chromatographic peaks of Figure 3 correspond to the three nonlinear trimers of Figure 5 and we assign the RT = 50 min peak as the 120° trimer which is the most abundant at lower temperatures. As the polymerization temperature ap-

proaches 150 °C, the decomposition temperature of the photopolymer,<sup>8</sup> reverse reactions may also occur, giving rise to a dynamic equilibrium of polymerization and depolymerization.<sup>7,8</sup> Under these conditions, most of the higher oligomers decompose and only the most stable isomers survive. Quantum chemical calculations predict the 60° close triangle as the most stable trimer,<sup>33</sup> so we assign the RT = 41 min peak to this isomer. Thus, the remaining RT = 47 min peak corresponds to the rectangular trimer. The assignment of the trimers indicates also some structural features of the tetramers. The two trimer fragments of the tetramers (Figure 2c) correspond to the rectangular and the 120° V-shaped isomers. According to the above model of bulk photopolymerization, these two fragments should come from at least two tetramers, because 90 and 120° interfullerene angles cannot be mixed in the same molecule (Figure 5). The significantly higher intensity of the rectangular trimer (Figure 2c) and its accumulation during the slow decomposition of the extract (Figure 2b) indicate that its parent tetramer corresponds to the most intensive RT = 78 min peak. The absence of linear trimer makes it more probable for the S-shaped and square tetramers to be assigned rather than the other two rectangular tetramers. Similar arguments suggest three different 120° tetramers (Figure 5) as possible parents of the minor decomposition product. The above assignments of trimers and tetramers are based on indirect evidence and cannot replace direct structural studies. Preparative HPLC separation and purification of the observed oligomers are in progress in order to determine their structures.

## 5. Summary

In summary, we have shown that bulk photopolymerization of C<sub>60</sub> gives rise to the formation of a solid solution of small oligomers with linear or planar structures. The crystal structure of the polymer remains fcc with a contracted lattice parameter relative to C<sub>60</sub>. The solvent-free dimer phase with a fcc structure can be crystallized from toluene. Detailed HPLC analysis and topochemical considerations show that V-shaped or triangle trimers are the major soluble oligomer components, depending on the temperature of polymerization.

**Acknowledgment.** This work was supported by the Hungarian Research Fund OTKA: T032613, T046700, and T043494.

## References and Notes

- (1) Rao, A. M.; Zhou, P.; Wang, K.-A.; Hager, G. T.; Holden, J. M.; Wang, Y.; Lee, W.-T.; Bi, X.-X.; Eklund, P. C.; Cornett, D. S.; Duncan, M. A.; Amster, I. J. *Science* **1993**, 259, 955.
- (2) Zhou, P.; Dong, Z.-H.; Rao, A. M.; Eklund, P. C. *Chem. Phys. Lett.* **1993**, 211, 337.
- (3) For a review, see: Eklund, P. C.; Rao, A. M., Eds. *Fullerene Polymers and Fullerene Polymer Composites*; Springer: Berlin, 2000.
- (4) Eklund, P. C.; Rao, A. M.; Zhou, P.; Wang, Y.; Holden, J. M. *Thin Solid Films* **1995**, 257, 185.
- (5) Wang, Y.; Holden, J. M.; Dong, Z.-H.; Bi, X.-X.; Eklund, P. C. *Chem. Phys. Lett.* **1993**, 211, 341.
- (6) Itchkawitz, B. S.; Long, J. P.; Schedel-Niedrig, T.; Kabler, M. N.; Bradshaw, A. M.; Sclögl, R.; Hunter, W. R. *Chem. Phys. Lett.* **1995**, 243, 211.
- (7) Sakai, M.; Ichida, M.; Nakamura, A. *Chem. Phys. Lett.* **2001**, 335, 559.
- (8) Wang, Y.; Holden, J. M.; Bi, X.-X.; Eklund, P. C. *Chem. Phys. Lett.* **1994**, 217, 413.
- (9) Pederson, M. R.; Quong, A. A. *Phys. Rev. Lett.* **1994**, 74, 2319.
- (10) Adams, G. B.; Page, J. B.; Sankey, O. F.; O'Keeffe, M. *Phys. Rev. B* **1994**, 50, 17471.
- (11) Porezag, D.; Pederson, M. R.; Frauenheim, Th.; Köhler, T. *Phys. Rev. B* **1995**, 52, 14963.
- (12) Porezag, D.; Pederson, M. R.; Frauenheim, Th.; Köhler, T. *Carbon* **1997**, 37, 463.
- (13) Porezag, D.; Jungnickel, G.; Frauenheim, Th.; Seifert, G.; Ayuela, A.; Pederson, M. R. *Appl. Phys. A* **1997**, 64, 321.
- (14) Lee, K. H.; Eun, H. M.; Park, S. S.; Suh, Y. S.; Jung, K.-W.; Lee, S. M.; Lee, Y. H.; Osawa, E. *J. Phys. Chem. B* **2000**, 104, 7038.
- (15) Adams, G. B.; Page, J. B. *Phys. Status Solidi B* **2001**, 226, 95.
- (16) Burger, B.; Winter, J.; Kuzmany, H. *Z. Phys. B* **1996**, 101, 227.
- (17) Burger, B.; Kuzmany, H.; Nguyen, T. M.; Sitter, H.; Walter, M.; Martin, K.; Müllen, K. *Z. Phys. B* **1996**, 101, 227.
- (18) Hassanien, A.; Gasperic, J.; Demsar, J.; Musevic, I.; Mihailovic, D. *Appl. Phys. Lett.* **1997**, 70, 417.
- (19) Onoe, J.; Takeuchi, K. *Phys. Rev. Lett.* **1997**, 79, 2987.
- (20) Sun, Y.-P.; Ma, B.; Bunker, C. E.; Liu, B. *J. Am. Chem. Soc.* **1995**, 117, 12705.
- (21) Ma, B.; Milton, A. M.; Liu, B.; Sun, Y.-P. *Chem. Phys. Lett.* **1998**, 288, 854.
- (22) Cataldo, F. *Polym. Int.* **1999**, 48, 143.
- (23) Cataldo, F. *Eur. Polym. J.* **2000**, 36, 653.
- (24) Pusztai, T.; Oszlányi, G.; Faigel, G.; Kamarás, K.; Gránásky, L.; Pekker, S. *Solid State Commun.* **1999**, 111, 595.
- (25) Wang, G.-W.; Komatsu, K.; Murata, Y.; Shiro, M. *Nature* **1997**, 387, 583.
- (26) Iwasa, Y.; Tanoue, K.; Mitani, T.; Izuoka, A.; Sugawara, T.; Yagi, T. *Chem. Commun.* **1998**, 1411.
- (27) Komatsu, K.; Wang, G.-W.; Murata, Y.; Tanaka, T.; Fujiwara, K.; Yamamoto, K.; Saunders, M. *J. Org. Chem.* **1998**, 63, 9358.
- (28) Ohtsuki, T.; Masumoto, K.; Tanaka, T.; Komatsu, K. *Chem. Phys. Lett.* **1999**, 300, 661.
- (29) Komatsu, K.; Fujiwara, K.; Murata, Y. *Chem. Lett.* **2000**, 1016.
- (30) Fujitsuka, M.; Luo, C.; Ito, O.; Murata, Y.; Komatsu, K. *J. Phys. Chem. A* **1999**, 103, 7155.
- (31) Komatsu, K.; Fujiwara, K.; Tanaka, T.; Murata, Y. *Carbon* **2000**, 38, 1529.
- (32) Fujitsuka, M.; Fujiwara, K.; Murata, Y.; Uemura, S.; Kunitake, M.; Ito, O.; Komatsu, K. *Chem. Lett.* **2001**, 384.
- (33) Kunitake, M.; Uemura, S.; Ito, O.; Fujiwara, K.; Murata, Y.; Komatsu, K. *Angew. Chem., Int. Ed.* **2002**, 41, 969.
- (34) Pekker, S.; Kamarás, K.; Kovács, É.; Pusztai, T.; Oszlányi, G. *Synth. Met.* **2001**, 121, 1109.
- (35) Pekker, S.; Kovács, É.; Kamarás, K.; Pusztai, T.; Oszlányi, G. *Synth. Met.* **2003**, 133–134, 685.
- (36) Moret, R.; Launois, P.; Wagberg, T.; Sundqvist, B.; Agafonov, V.; Davydov, V. A.; Rakhmanina, A. V. *Eur. Phys. J. B* **2004**, 37, 25.
- (37) Fast, D. J. *Entropy*; Philips Technical Library: Eindhoven, The Netherlands, 1962; p 156.